

Electronic Structure of Disordered Alloys—Iteration Scheme Converging to the Coherent-Potential Approximation

An-Ban Chen*

Department of Physics, College of William and Mary, Williamsburg, Virginia 23185

An iteration scheme (referred to as IATA) that repeatedly uses the average- t -matrix approximation (ATA) will be examined. The objective of this work is to devise a computational method which will permit the coherent-potential approximation (CPA) to be applied with realistic alloy potentials. A numerical comparison is made between the IATA and two other schemes which are based on well-known self-energy expressions in a single-band model. The results indicate that among the three methods, the IATA is the only one which converges from the virtual-crystal limit toward CPA for all alloy parameters and for all energies inside the CPA band. However, in concentrated and strong-scattering alloys, especially for minority subbands where ATA is not at all trustworthy, IATA does not converge particularly fast and may produce unphysical structures in the intermediate iterations. A combination of IATA with the extrapolation methods speeds convergence, provides an easy way to achieve the CPA result, and is believed to be useful for calculations on realistic alloys. Finally, an IATA technique for muffin-tin potentials is developed.

I. INTRODUCTION

The application of the coherent-potential approximation^{1,2} (CPA) to more realistic potentials is one of the most urgent tasks today in the alloy theory. Although it has been a while since Soven³ proposed his formal CPA method for random muffin-tin potentials, to date there still exists no published computation using these more realistic potentials. This is due to the complicated nature of the CPA self-consistent solution (for transition-metal alloys with only the first three angular momentum phase shifts taken as nonvanishing, the CPA equation becomes a complicated 9×9 matrix equation with the unknown matrix appearing in a sum over the Brillouin zone). To circumvent this difficulty, Schwartz, Brouers, Vedyayev, and Ehrenreich⁴ (to be referred to as SBVE) reexamined the non-self-consistent average- t -matrix approximation⁵ (ATA) and compared ATA with CPA. They pointed out that in many cases ATA is almost identical to CPA, and is at least a good first approximation in an iteration scheme leading to the self-consistent CPA solution. Therefore, their work implies that an iteration of ATA (referred to as IATA) would provide a means of solving the CPA self-consistent problem. This work is intended to examine the applicability of IATA, and then to develop a formalism to apply it to muffin-tin potentials.

The paper begins with a description of IATA. We then examine the numerical results of IATA in a single-band model. It will be seen that a direct IATA starting with the virtual crystal² will finally lead to the CPA solution for all energies in the CPA band. For comparison, two other iteration methods are given based on two well-known self-energy expressions which are consistent with the CPA equation but are shown not to converge to CPA for many

cases. In many cases where ATA is not at all trustworthy, a number of iterations are required by IATA to converge to the CPA result, and in the intermediate iterations very unphysical structures are produced in the density of states. Thus, a direct IATA scheme starting from the virtual crystal for all energies in the band may not be practical for a realistic calculation.

However, when a simple extrapolation method is incorporated in the ATA iteration, the speed of convergence is greatly improved so that it should make the method practical. Besides, since the ATA iteration converges at all energy points of interest and for all alloy parameters, it can be used to generate the correct CPA self-energies at a few energy points. These self-energies can then be used to extrapolate to the initial self-energies for a ATA iteration at neighboring energies in the band. In this way, the ATA iterations may be used to obtain the CPA result throughout the band.

Since our primary goal is to work with more realistic potentials, an ATA iteration scheme for muffin-tin potentials is presented in Sec. IV.

II. SINGLE-SITE APPROXIMATION AND ITERATION SCHEME

The single-site approximation (SSA) in the Green's function formalism for disordered alloys has been discussed many times in the literature.^{2,4} In this section we will briefly define the quantities employed in the formalism and quote some of the SSA results that are to be used in the present work.

Let the one-electron Hamiltonian H be composed of a periodic part W and a random part U . The Green's function $G(z)$ is defined in terms of H by $G(z) \equiv (z - H)^{-1}$. We are interested in the ensemble-averaged Green's function $\langle G(z) \rangle$. This quantity determines many of the static electronic properties such as the density of states. For the present pur-

pose the operation $\langle \rangle$ is taken to be the so-called configurational average which is an average over all the possible arrangements of atoms on the lattice sites. Since $\langle G(z) \rangle$ has the crystal translational symmetry, a periodic self-energy operator $\hat{\sigma}$ can be defined such that

$$\langle G(z) \rangle = (z - W - \hat{\sigma})^{-1}. \quad (2.1)$$

It is useful to write down the exact expression for $\hat{\sigma}$ in terms of a periodic reference Green's function $\tilde{G} = (z - W - \tilde{\sigma})^{-1}$,

$$\hat{\sigma} = \tilde{\sigma} + \langle T \rangle (1 + G \langle T \rangle)^{-1}, \quad (2.2)$$

where the T operator is defined as

$$T = (U - \tilde{\sigma}) [1 - \tilde{G}(U - \tilde{\sigma})]^{-1}. \quad (2.3)$$

The problem is then reduced to the determination of $\langle T \rangle$ or $\hat{\sigma}$.

In order to employ the SSA the random potential is assumed to be decomposable into localized site contributions, i. e., $U = \sum_n U_n$. With this the T operator of Eq. (2.3) can be expanded in series of the products of the atomic t operators, the so-called multiple-scattering expansion. The SSA consists of the neglect of the statistical correlations between the atomic t operator at a given site and the effective wave coming to that site.^{2,4,6} As a consequence of the SSA, $\hat{\sigma}$ can be decomposed into site contributions, $\hat{\sigma} = \sum_n \hat{\sigma}_n$, with⁷

$$\hat{\sigma}_n = \tilde{\sigma}_n + \langle T_n \rangle (1 + G_n \langle T_n \rangle)^{-1}, \quad (2.4)$$

where $\tilde{\sigma}_n$ is the reference self-energy at site n , G_n is the projection of \tilde{G} onto the local region of U_n , and T_n is the atomic t operator associated with the site n . The operator T_n is given by the same equation as for T , i. e., Eq. (2.3) with U and $\tilde{\sigma}$ replaced by U_n and $\tilde{\sigma}_n$, respectively. Equation (2.4) serves as the starting point for the present work.

As has already been pointed out in SBVE, Eq. (2.4) can be used in two ways. First, as a self-consistent version, the reference self-energy can be adjusted such that there is no further self-energy correction in the SSA, i. e.,

$$\langle T_n \rangle = 0, \quad (2.5)$$

which is the coherent-potential approximation and is considered as the best single-site approximation.⁸ Second, the non-self-consistent version of Eq. (2.4), the ATA, gives a correction to the reference self-energy.

There is a further use of Eq. (2.4). Since CPA is computationally much more difficult than ATA, Eq. (2.4) can be used as an iteration scheme to find a succession of self-energy corrections in the hope that the CPA self-consistency will be achieved. I shall refer to this iteration scheme as IATA, which stands for the iterative average- t -matrix approximation. Explicitly, IATA takes the form

$$\begin{aligned} \sigma_n^{(i+1)} &= \sigma_n^{(i)} + [1 + \langle T_n^{(i)} \rangle G_n^{(i)}]^{-1} \langle T_n^{(i)} \rangle \\ &\equiv K(\sigma_n^{(i)}), \end{aligned} \quad (2.6)$$

where $\sigma_n^{(i)}$ refers to the n th-site self-energy obtained in the i th iteration, with similar interpretations for $T_n^{(i)}$ and $G_n^{(i)}$.

We note that in Eq. (2.6) all the quantities involved, $\sigma_n^{(i)}$, $T_n^{(i)}$, and $G_n^{(i)}$, are all confined to the local region of U_n . They are also functions of the same energy. Thus, in all stages of iteration, the self-energy computed at a site, for a given energy, is independent of the behavior of $\sigma_n^{(i)}$, $T_n^{(i)}$, and $G_n^{(i)}$, belonging to other sites or other energies. In Sec. III the numerical results of the IATA for a single-band model will be discussed.

III. NUMERICAL RESULTS FOR A SINGLE-BAND MODEL

In this section, we shall numerically examine the IATA in a single-band model,¹ where the CPA equation is easy to solve, and the CPA results are well known.^{2,4,6} In spite of the mathematical simplicity of this model, it does contain some features of an alloy band. A detailed investigation of the numerical results from this simple model will give us insight into the more complicated realistic systems. In what follows, we will first consider the IATA starting with the virtual-crystal approximation and will compare the result with that for the CPA. The IATA will then be compared with two other iteration schemes that are trivially deduced from the CPA equation. Lastly, we shall discuss a combination of IATA and an extrapolation method which converges to the CPA result with less iterations.

The single-band-model Hamiltonian for a disordered substitutional alloy $A_x B_y$ ($x + y = 1$) has the form

$$H = W + U = \sum'_{n,m} |n\rangle b_{nm} \langle m| + \sum_n |n\rangle \epsilon_n \langle n|, \quad (3.1)$$

where W , off-diagonal in the Wannier basis $\{|n\rangle\}$, is assumed to be periodic and U is site diagonal but is random. ϵ_n takes on values ϵ_A or ϵ_B depending on whether an A atom or a B atom is at site n . For convenience, we shall use the half-bandwidth w associated with the periodic band as the energy unit, i. e., $w = 1$, and define a scattering strength δ such that $\epsilon_A = -\epsilon_B = \frac{1}{2}\delta$.

As is well known, for a single-band CPA calculation the only input needed from the pure crystal is the density of states, which we shall assume to be elliptical, i. e.,

$$\pi \rho_0(E) = 2(1 - E^2)^{1/2}. \quad (3.2)$$

The CPA self-energy σ_{CPA} then satisfies a cubic equation⁹ from which the correct roots can be determined easily. The alloy density of states per atom $\rho(E)$ is then calculated by taking the imagi-

mary part of the site-diagonal Green's-function matrix element F ,

$$\rho(E) = \pm (1/\pi) \text{Im} F(E \mp i0, \sigma_{\text{CPA}}), \quad (3.3)$$

where

$$\begin{aligned} F(z, \sigma) &\equiv \langle 0 | (z - W - \sigma)^{-1} | 0 \rangle \\ &= 2(z - \sigma) - 2[(z - \sigma)^2 - 1]^{1/2}. \end{aligned} \quad (3.4)$$

The IATA equation (2.6) in the present model also becomes a scalar iteration,

$$\sigma^{(i+1)} = \sigma^{(i)} + t^{(i)} (1 + F^{(i)} t^{(i)})^{-1}, \quad (3.5)$$

where the averaged atomic- t -matrix element $t^{(i)}$ is explicitly given by

$$t^{(i)} = \frac{\epsilon - \sigma^{(i)} + [\delta^2/4 - (\sigma^{(i)})^2] F^{(i)}}{1 + 2\sigma^{(i)} F^{(i)} - [\delta^2/4 - (\sigma^{(i)})^2] (F^{(i)})^2}. \quad (3.6)$$

Here $F^{(i)}$ is $F(z, \sigma^{(i)})$ defined in Eq. (3.4), and $\epsilon \equiv x\epsilon_A + y\epsilon_B$ is the averaged potential strength.

Now, let us discuss the IATA starting with the virtual crystal, i. e., $\sigma^{(0)} = \epsilon$. In SBVE, the ATA (the first iteration in IATA) and the CPA density of states for some alloys were compared. It was found that for the weak-scattering ($\delta \ll 1$) and low-concentration ($x \ll 1$) cases, ATA and CPA are almost identical. We find that in one or two iterations the IATA converges very well to the CPA. However, it should be emphasized that ATA is not adequate for many cases, especially for concentrated, strong-scattering alloys. Figure 1(a) shows that the ATA density of states for an alloy with $x = 0.5$ and $\delta = 0.8$ is quite different from the CPA result. But a single further iteration brings IATA very close to CPA, and excellent visual con-

vergence is achieved in less than ten iterations [a more precise convergence criterion for this case will be discussed later; see Fig. 2(a)]. Figure 1(b) is the case of a concentrated ($x = 0.5$) and very-strong-scattering ($\delta = 2.0$) alloy. ATA is least trustworthy for this case. Further iterations show that IATA gradually converges to CPA. The cusps of the bare Green's function persist in the intermediate iterations but gradually disappear. Figure 1(c) is the density of states for an alloy in the split-band case ($\delta = 1.5$) with a minority subband ($x = 0.15$). Since ATA is very similar to CPA in the majority subband, only a few iterations are needed to achieve convergence in this subband. But caution must be exercised for the minority subband. In the intermediate steps of the iteration, IATA may produce very unphysical structures in the density of states, e. g., there are wiggles in the density of states in the tenth iteration as shown in the figure. Similarly, in the second iteration which is not shown in the figure the IATA density of states has two sharp spikes for the minority subband. Note also that although final convergence is achieved, the convergence is not rapid in this subband (60 iterations are needed for visual convergence).

In SBVE, ATA and CPA are also compared in a two-band model. They pointed out that ATA is a good approximation to CPA in all dilute alloys with parameters appropriate to transition- and noble-metal alloys. But in concentrated alloys, ATA fails in the energy regions between the two d subbands. In a modified two-band-model calculation,¹⁰ a direct IATA from the virtual crystal has been employed to obtain the self-energy. The

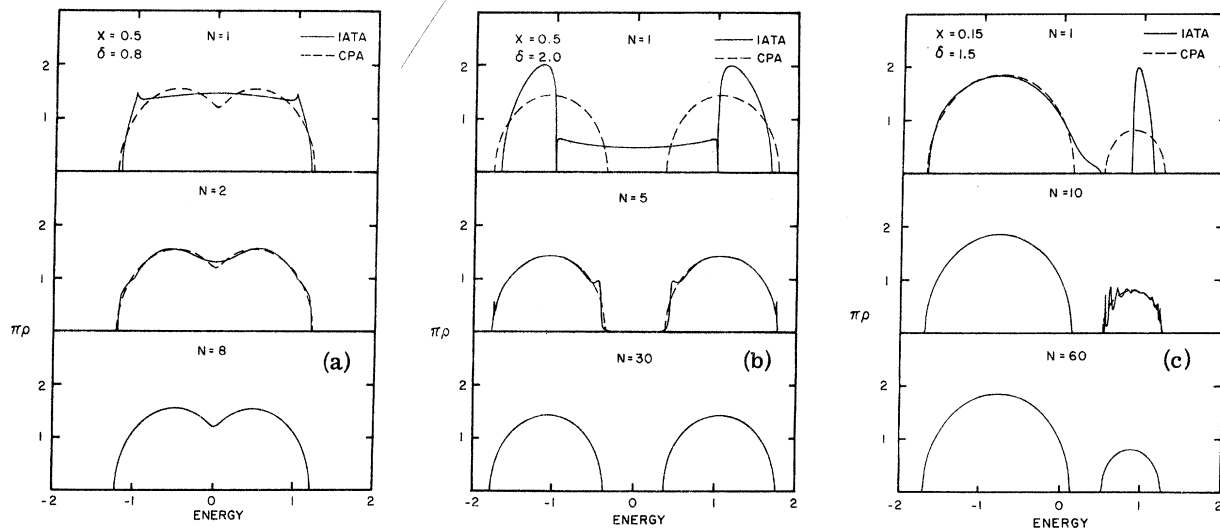


FIG. 1. Comparison of the density of states calculated in the IATA and the CPA for three alloys: (a) $x = 0.5$, $\delta = 0.8$; (b) $x = 0.5$, $\delta = 2.0$; (c) $x = 0.15$, $\delta = 1.5$. In each graph, N indicates the number of iterations in IATA. Note that energies are normalized to the half-bandwidth w , and hence are in dimensionless units.

speed of convergence to CPA is found to be very fast for all cases with parameters appropriate to transition- and noble-metal alloys. The reason for the improvement of ATA and for the fast convergence in IATA in the two-band models is that, in these models, the d bands are hybridized with the conduction band. This produces a very broad base in the pure constituent d -band density of states. Thus, the energy separation between the d -band centers of the two alloy constituents is never large enough to produce a split d band in the alloy. The most severe cases in the two-band models are only equivalent to the moderately-strong-scattering cases ($0.5 < \delta < 1.0$) of the single-band model [see Fig. 1(a)].

Some conclusions can be drawn from the above result. For weak-scattering alloys, ATA is an excellent approximation to CPA. For concentrated alloys with moderately-strong-scattering strengths, ATA is not adequate, but IATA converges easily to CPA. In concentrated, strong-scattering alloys, or in a split minority subband, where ATA is not trustworthy, a direct IATA from the virtual crystal is not fast and furthermore, unphysical structures may appear in the density of states in the intermediate iterations.

The densities of states of real noble and transition metals are quite complex. For an alloy composed of these metals, the important energy widths are those of the spikes in the density of states. Therefore, one tends to think of noble- and transition-metal alloys as strong-scattering alloys. Thus, ATA will not give accurate structures in the density of states for those alloys when they are concentrated. Also, a direct IATA from the virtual crystal may not be practical, since many iterations are required and in each iteration, as we shall see, there are lengthy mathematical manipulations involved.

One point should be emphasized. For the cases tested, IATA converges to CPA for all energies of interest and for all alloy parameters. This convergence is important since there are numbers of trivial iteration schemes that can be set up from the CPA equation with, however, no theory to guarantee their convergence.

Next, we shall compare the IATA with the other two iteration schemes which are based on the two well-known self-energy expressions, namely, the Soven's CPA equation,¹¹

$$\sigma_n = \bar{U}_n - (U_n^A - \sigma_n) \bar{G} (U_n^B - \sigma_n), \quad (3.7)$$

and the self-energy for the dilute scatters,

$$\sigma_n = \bar{\sigma}_n + \langle T_n \rangle. \quad (3.8)$$

In Eq. (3.8) the correction to the self-energy is just the averaged atomic t operator. This equation can be obtained if in the average of the total T

operator in Eq. (2.3) each atomic t operator is replaced by its averaged $\langle T_n \rangle$, and "exclusions" in the summation are neglected in every term of the multiple-scattering series for T of Eq. (2.3).¹² If we treat Eqs. (3.7), (3.8), and the ATA equation (2.4) as self-consistent equations, they are consistent with the CPA equation $\langle T_n \rangle = 0$. In particular, the self-consistent version of the ATA equation in the single-band model reduces to Onda and Toyozawa's¹³ equation,

$$\sigma = \epsilon + \chi y \delta^2 F [1 + (\epsilon + \sigma) F]^{-1}. \quad (3.9)$$

However, considered as iteration equations, Eqs. (3.7) and (3.8) are, in fact, different from the IATA. We shall refer to the iterations of Eqs. (3.7) and (3.8) as ICPS and ICPT, respectively. All of the three iterations can be put into the same form $\sigma_n^{(i+1)} = \kappa(\sigma^{(i)})$, but with different functional forms for κ . Explicitly, for ICPS,

$$\kappa(\sigma^{(i)}) = \bar{U}_n - (U_n^A - \sigma_n^{(i)}) G_n^{(i)} (U_n^B - \sigma_n^{(i)}), \quad (3.10)$$

and for ICPT,

$$\kappa(\sigma_n^{(i)}) = \sigma_n^{(i)} + \langle T_n^{(i)} \rangle. \quad (3.11)$$

For IATA, $\kappa(\sigma_n^{(i)})$ is given by the right-hand side of Eq. (2.6).

Now, let us compare the numerical results of the three schemes. Figure 2(a) is a plot of the number of iterations needed as a function of energy for the self-energy to converge to CPA to a part in 10^{-4} of the half-bandwidth, i. e., $|\sigma^{(i)} - \sigma_{\text{CPA}}| < 10^{-4}$, for an alloy with $\chi = 0.5$ and $\delta = 0.8$. The starting self-energy in each of the three cases is the virtual-crystal self-energy, i. e., $\sigma^{(0)} = \epsilon$. We see that all three methods are convergent in this alloy. The more interesting and important point we want to stress is not the speed of the convergence with IATA but the fact that it does so for a wide range of the parameters δ and χ . We found that IATA always converges for all significant energies. We must, of course, exclude those energies for which the CPA self-energy has a pole,² but at those energies the density of states is zero, so that they are physically insignificant. In contrast, ICPT and ICPS fail to converge to CPA for many cases, especially for those cases where the CPA results are really important. For example, in the alloy $\chi = 0.5$, $\delta = 2.0$, both the ICPT and ICPS self-energies diverge at all energy points inside the band. For the alloy with $\chi = 0.15$ and $\delta = 1.5$ [see the density of states in Fig. 1(c)], ICPT fails to converge for the energy region inside the minority subband and ICPS, although it converges in the minority subband, strangely fails to converge in the majority subband. This kind of behavior occurs even in the dilute and non-split-band case. For example, in Fig. 2(b), we show that for the alloy with $\chi = 0.1$ and $\delta = 0.8$, IATA is always convergent, while

ICPT and ICPS may fail in some energy ranges.

Thus, among the three iteration schemes we have investigated, only IATA is completely reliable. Although we cannot prove analytically that this iteration of a non-self-consistent approximation converges to the corresponding self-consistent result, the evidence we have supports this conclusion. Recall that what we have done in each iteration of the IATA is to make the single-site approximation (SSA) and then sum up the multiple-scattering series exactly to obtain the self-energy correction. By contrast in ICPS and ICPT schemes, further approximations in the summation of the multiple-scattering series in addition to the SSA are required to obtain the κ 's given in Eqs. (3.10) and (3.11). A similar conclusion would hold for any other possible iteration schemes that could be trivially derived from the CPA equation $\langle T_n \rangle = 0$.

As more severe tests of the IATA, some very inaccurate initial self-energies were deliberately used in the iteration for several cases. The interesting result of this study is that IATA converges for these choices roughly at the same speed as when one starts with the virtual crystal. On the other hand, the ICPS and ICPT fail to converge in all the drastic tests.

The above suggests that the IATA can be used in two ways. For those cases in which a direct application of the IATA from the virtual crystal converges sufficiently rapidly, it can be used to obtain the CPA results throughout the band. For those cases where a direct application of the scheme is impractically slow, it can be used to generate a few CPA results for several energies in the band. Then an extrapolation method combined with the IATA can be employed to obtain the results for the remainder of the band.

A simple application of Newton's extrapolation method to obtain an initial self-energy for IATA at a given energy from CPA values for two neighboring energies suffices to improve the rate of convergence dramatically. This kind of extrapolation method has been tested on the single-band model. With an energy interval of 0.001, a convergence radius of 10^{-4} in self-energy, i. e., $|\sigma^{(i)} - \sigma_{\text{CPA}}| < 10^{-4}$, is obtained in only a few iterations of IATA for all alloy cases including the difficult cases of Figs. 1(b) and 1(c). In this extrapolation method, ICPT gives similar results as IATA, but ICPS does not always converge to the CPA result. In other words, although ICPT is likely to break down with a bad initial self-energy, it works well when the initial self-energy is close to the CPA result. In contrast, for some cases ICPS may yield an iterated self-energy further away from the CPA value than the initial value even when the initial self-energy is very close to the CPA value.

In the above, a sample iteration technique was used to solve an equation $\sigma = K(\sigma)$. The convergence for this procedure is at best geometrical.

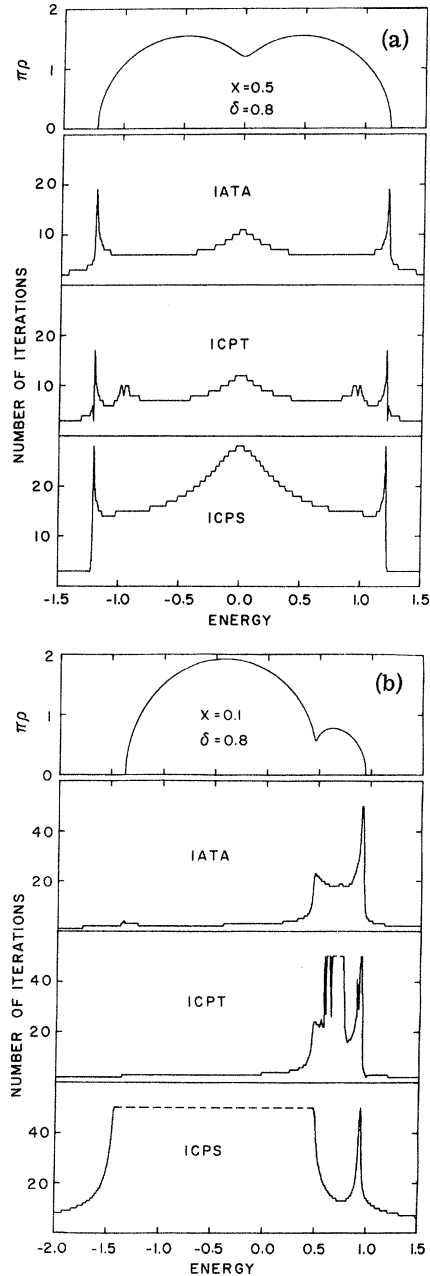


FIG. 2. Comparison of the convergence for three iteration schemes IATA, ICPT, and ICPS. The numbers of iterations needed to make the self-energy correct to 10^{-4} , i. e., $|\sigma^{(i)} - \sigma_{\text{CPA}}| < 10^{-4}$, are plotted as a function of the energy for two alloys: (a) $x=0.5$, $\delta=0.8$; (b) $x=0.1$, $\delta=0.8$. On top of each graph is the plot of the CPA density of states as a function of the energy. Note that the dashed lines indicate the energy regions where the methods do not converge. The energies are normalized to the half-bandwidth w , and hence are in dimensionless units.

TABLE I. Number of iterations required for σ to converge to $|\sigma - \sigma_{\text{CPA}}| < 10^{-4}$ from the virtual-crystal value.

χ	δ	Energy	IATA	EIATA	ICPT	EICPT	ICPS	EICPS
0.5	0.8	-0.60	7	4	8	7	18	7
0.5	0.8	0.00	12	5	13	6	29	7
0.5	2.0	0.40	53	8	>61	19	>61	>61
0.5	2.0	1.00	11	6	>61	>61	>61	>61
0.15	1.5	-1.00	4	4	5	6	>71	7
0.15	1.5	0.50	19	56	21	>71	>71	63
0.15	1.5	1.00	26	8	>71	32	14	>71
0.1	0.8	-0.50	3	3	4	4	>51	5
0.1	0.8	0.48	24	8	25	8	>51	15
0.1	0.8	0.90	31	9	34	9	23	10

In the vicinity of an exact solution, a more rapid convergence can usually be achieved by using an extrapolation method. For example, with two estimated values σ_1 and σ_2 , an improved σ can be obtained from the linear extrapolation equation

$$\sigma = K(\sigma_1) + \frac{K(\sigma_2) - K(\sigma_1)}{\sigma_2 - \sigma_1} (\sigma - \sigma_1). \quad (3.12)$$

With more estimated values for σ , Eq. (3.12) can be further improved by using a higher-order extrapolation method.¹⁴ However, if the estimated values are far from the exact solution, a single extrapolation usually will not provide an accurate solution. But if the extrapolation procedure is iterated, it often exhibits a convergence more rapid than the simple-iteration technique. A higher-order extrapolation method in general exhibits a more rapid convergence, especially when the function K is a smooth function. As a test of this extrapolation-iteration procedure, the linear equation (3.12) will be applied to the three $K(\sigma)$'s given in Eqs. (2.6), (3.10), and (3.11). We shall refer to these three extrapolation-iteration schemes as EIATA, EICPS, and EICPT, respectively.

A summary of the convergence of the extrapolation-iteration schemes as compared to the simple iteration schemes is given in Table I. The integer numbers in the table are the number of iterations that are required for σ to converge to the CPA value to an accuracy of 10^{-4} , i. e., $|\sigma^{(i)} - \sigma_{\text{CPA}}| \leq 10^{-4}$. The alloy parameters are the same as those used in the previous discussions. For a better understanding of the table, the reader should refer to the corresponding CPA density of states in Figs. 1 or 2 for each case. We see that the convergence for these extrapolation-iteration schemes is in general better than that for the simple-iteration procedures. Among the three extrapolation-iteration schemes, EIATA is the only one that converges at all energies and for all alloy parameters. This result further supports our confidence in the iteration using the ATA. A more detailed comparison reveals that except for one case ($\chi = 0.15$, $\delta = 1.5$, $E = 0.5$), the EIATA is a great improvement over IATA in convergence. For all energies inside the

CPA band, EIATA requires less than ten iterations to achieve an excellent convergence. We feel that with this rate of convergence, realistic calculations are feasible. We note that the exceptional case corresponds to an energy in the gap of a split CPA band [see Fig. 1(c)]. We also note that the virtual-crystal and the ATA self-energies deviate very much from the CPA values in strong-scattering alloys, especially around the energy¹⁵ $E = -\epsilon = -(x\epsilon_A + y\epsilon_B)$ (for the exceptional case, the energy $E = 0.5$ is close to $-\epsilon = 0.525$; the three self-energies are $\sigma^{(0)} = \epsilon = -0.525$, $\sigma^{(1)} = \sigma_{\text{ATA}} = -1.2$, and $\sigma_{\text{CPA}} = -4.1233$). Thus, the slow convergence of the EIATA for this case is due to the fact that bad initial values are used in a linear extrapolation scheme which causes some random searches before reaching the solution. However, in many cases the self-energy in the band gap has no physical significance so the calculational difficulties associated with this energy region can be avoided. We can also improve the initial self-energies by energy extrapolation. More precisely, once the CPA self-energies have been obtained at several energies inside the band, energy extrapolations can be employed to obtain better initial self-energies than the virtual-crystal values for an EIATA iteration at the neighboring energies. In this way, the calculation can be extended from the band to the band gaps. Furthermore, a higher-order extrapolation method can also be incorporated in the iteration scheme to speed the convergence.

In summary, the numerical results presented in this section suggest that the ATA iteration along with the extrapolation methods may provide a means of calculating the CPA electronic structure of a realistic alloy. In Sec. IV, an ATA iteration method for muffin-tin potentials will be discussed.

IV. APPLICATION OF ITERATION METHOD TO RANDOM MUFFIN-TIN POTENTIALS

In this section the IATA is applied to random muffin-tin potentials. It can be seen from Eq. (2.4) that by working in coordinate space one could take advantage of the localization of the potential. Because of this it is easy to apply the IATA to Soven's formalism³ for muffin-tin potentials. Soven transforms the problem from one with the original muffin-tin potentials to one with spherically symmetric δ -shell potentials. The density of states for the muffin-tin potentials can be found in terms of the solution to the δ -shell-potential problem. Many of the formulas used in this section come from Soven's work. For detail derivations the reader should refer to his paper.

Consider a binary alloy $A_x B_x$ containing N atoms in a volume Ω with muffin-tin potentials \bar{V}_A and \bar{V}_B randomly distributed on lattice sites. The poten-

tials \bar{V}_A and \bar{V}_B are characterized by a common muffin-tin radius R and their logarithmic derivatives $\bar{\gamma}_l^{A,B}(E)$ at R for angular momentum l and energy E . The δ -shell potentials V_A and V_B that Soven used can be defined by the following coordinate matrix element of these potentials at site zero (S. 9),¹⁶

$$V_{A,B}(\vec{r}, \vec{r}') = \sum_{LL'} Y_L(\hat{r}) \frac{\delta(r-R)}{R^2} W_{LL'}^{A,B} \times \frac{\delta(r'-R)}{R^2} Y_{L'}(\hat{r}'), \quad (4.1)$$

where the set $\{Y_L\}$ are orthonormalized real spherical harmonics and L includes the principal angular momentum quantum number l and other degeneracy indices of l .¹⁷ The potential strength parameters $W_{LL'}^{A,B}$ are chosen such that each δ -shell potential has the same phase shifts as its corresponding muffin-tin potential. The $W_{LL'}^{A,B}$ are given by (S. 10)

$$W_{LL'}^{A,B} = W_L^{A,B} \delta_{LL'}, \\ = R^2 [\bar{\gamma}_l^{A,B}(E) - \kappa j'_l(\kappa R) / j_l(\kappa R)] \delta_{LL'}, \quad (4.2)$$

where $\kappa^2 \equiv E$, j_l is the regular spherical Bessel function, and j'_l its derivative. Since the potentials in Eq. (4.1) are localized on spherical shells, the single-site self-energies according to Eq. (2.4) are also localized on spherical shells. Thus, the coordinate matrix element of the CPA self-energy $\hat{\sigma}_0$ for the lattice site located at the origin takes the form (S. 21)

$$\sigma_0(\vec{r}, \vec{r}') = \sum_{LL'} Y_L(\hat{r}) \frac{\delta(r-R)}{R^2} W_{LL'} \frac{\delta(r'-R)}{R^2} Y_{L'}(\hat{r}'). \quad (4.3)$$

Then Soven was able to obtain the CPA density of states associated with the random muffin-tin potentials in terms of the parameters characterizing the δ -shell potentials. The formal result is (S. 41),

$$\pi\rho(E) = -\text{Im} \sum_k \sum_{LL'} \frac{\partial P_{LL'}^k}{\partial E} [W(1 - P^k W)^{-1}]_{LL'}, \\ -N \text{Im} \sum_{LL'} G_{L'L} \left(x \frac{dW_L^A}{dE} [1 - (W^A - W)G]_{LL'}^{-1} \right. \\ \left. + y \frac{dW_L^B}{dE} [1 - (W^B - W)G]_{LL'}^{-1} \right), \quad (4.4)$$

where the sum over the wave vector k extends over the first Brillouin zone and P^k [referred to as the Korringa-Kohn-Rostoker (KKR) Green's function matrix] is defined by (S. 43)

$$P_{LL'}^k \equiv \kappa j_l(\kappa R) n_l(\kappa R) \delta_{LL'} + i^{l-l'} j_l(\kappa R) j_{l'}(\kappa R) B_{LL'}^k, \quad (4.5)$$

with $B_{LL'}^k$ being the structure factor in the KKR¹⁸ Green's function and n_l being an irregular spherical

Bessel function. In Eq. (4.4), P^k , W , G , etc., are matrices whose matrix elements are indexed by the quantum numbers L , e. g., $P_{LL'}^k$ is the LL' matrix element of P^k . The matrix element $W_{LL'}$ has been defined in Eq. (4.3) and G is closely related to the CPA Green's function [see Appendix A, Eq. (A7)] and is totally determined by P^k and W [also see (S. 34)],

$$G = \frac{1}{N} \sum_k P^k (1 - W P^k)^{-1}. \quad (4.6)$$

Thus, once the CPA self-energy or W is determined, the alloy density of states is obtained from Eq. (4.4). The matrix W satisfies the following equation (S. 24):

$$W = \bar{W} - (W^A - W)G(W^B - W), \quad (4.7)$$

where $\bar{W} = xW^A + yW^B$. Note that with only the first three angular momentum phase shifts taken to be nonvanishing, one needs to solve a 9×9 matrix equation for W . The unknown matrix W is contained in G , which involves a Brillouin sum as indicated in Eq. (4.6).¹⁹ Therefore, a formal solution of Eqs. (4.6) and (4.7) is possible but by no means trivial. If we want to use Eq. (4.7) as the basis for an iteration scheme, we would, presumably, encounter the same difficulties exhibited by ICPS in the single-band model. Since we have learned from the single-band model that IATA along with the extrapolation method is capable of obtaining the CPA result, we have reason to believe that this method may also work for this more complicated case.

To apply the IATA to Soven's formalism is a straightforward matter. Let $\sigma_n^{(i)}$, $\langle T_n^{(i)} \rangle$, and $G_n^{(i)}$ denote, respectively, the self-energy, the averaged atomic t operator, and the averaged single-site Green's function at site n in the i th iteration of IATA. As in Eq. (4.3) the matrix element of $\sigma_0^{(i)}$ can be written

$$\sigma_0^{(i)}(\vec{r}, \vec{r}') = \sum_{LL'} Y_L(\hat{r}) \frac{\delta(r-R)}{R^2} W_{LL'}^{(i)} \times \frac{\delta(r'-R)}{R^2} Y_{L'}(\hat{r}'). \quad (4.8)$$

As proved in Appendix A, we can write

$$\langle T_0^{(i)}(\vec{r}, \vec{r}') \rangle = \sum_{LL'} Y_L(\hat{r}) \frac{\delta(r-R)}{R^2} T_{LL'}^{(i)} \times \frac{\delta(r'-R)}{R^2} Y_{L'}(\hat{r}'), \quad (4.9)$$

$$G_0^{(i)}(\vec{r}, \vec{r}') = \sum_{LL'} Y_L(\hat{r}) G_{LL'} Y_{L'}(\hat{r}'), \quad |r| = |r'| = R \quad (4.10)$$

where $G_{LL'}^{(i)}$ and $T_{LL'}^{(i)}$, or their corresponding matrices $G^{(i)}$ and $T^{(i)}$, are totally determined by the KKR Green's-function matrix P^k and the self-energy

matrix $W^{(i)}$, i. e.,

$$G^{(i)} = \frac{1}{N} \sum_k P^k [1 - W^{(i)} P^k]^{-1}, \quad (4.11)$$

$$T^{(i)} = xT_A^{(i)} + T_B^{(i)}, \quad (4.12)$$

with $T_A^{(i)}$ and $T_B^{(i)}$ being

$$T_{A,B}^{(i)} \equiv (W^{A,B} - W^{(i)}) [1 - G^{(i)} (W^{A,B} - W^{(i)})]^{-1}. \quad (4.13)$$

Finally, the iterated self-energy matrix is obtained by the IATA expression,

$$W^{(i+1)} = W^{(i)} + T^{(i)} [1 + G^{(i)} T^{(i)}]^{-1}. \quad (4.14)$$

The IATA iteration for muffin-tin potentials is thus a straightforward though nontrivial numerical problem. The inputs of the calculation are the scattering phase shifts (or, equivalently, the \bar{y}_1^A and \bar{y}_1^B). The transition from the IATA to the EIATA is made by generalizing Eq. (3.12) to the following equation:

$$W_{LL'}^{(i+1)} = K_{LL'}(W^{(i-1)}) + \frac{K_{LL'}(W^{(i)}) - K_{LL'}(W^{(i-1)})}{W_{LL'}^{(i)} - W_{LL'}^{(i-1)}} \times (W_{LL'}^{(i+1)} - W_{LL'}^{(i-1)}), \quad (4.15)$$

where the matrix $K(W^{(i)})$ is just the expression on the right-hand side of Eq. (4.14).

Of course, there are still many problems to be overcome in a realistic calculation. For example, the Green function of a real system is not a smooth function of energy but, in fact, has singularities as is reflected in the sharp structures in the density of states of the pure crystal. This may cause some difficulty in using the energy extrapolation. However, since the sharp structures that appear in the Green's function of the pure crystal tend to be smeared out in the alloys, this difficulty may be overcome by adjusting the energy increment in the extrapolation. Of course the calculation of the structure constants¹⁸ appearing in the KKR Green-function matrix [see Eq. (4.5)] and of the Brillouin sum in Eqs. (4.4) and (4.11) are by no means easy, but they are unavoidable. Once those difficulties are overcome, the calculation of the electronic structure in the CPA can be accomplished.

ACKNOWLEDGMENTS

I would like to thank Dr. A. Sher and Dr. B. Segall for their proofreading of this manuscript. I also acknowledge helpful conversations with Dr. G. Weisz and with Dr. J. S. Faulkner's group at the Oak Ridge National Laboratories.

APPENDIX A

(a) We want to show that for any operator \hat{O} whose matrix element has the form

$$O(\vec{r}, \vec{r}') = \sum_{LL'} Y_L(\hat{r}) \frac{\delta(r-R)}{R^2} O_{LL'} \frac{\delta(r'-R)}{R^2} Y_L(\hat{r}'), \quad (A1)$$

the matrix element of the product operator $\hat{O}\hat{A}\hat{O}$ takes the form

$$\langle \vec{r} | \hat{O}\hat{A}\hat{O} | \vec{r}' \rangle = \sum_{LL'} Y_L(\hat{r}) \frac{\delta(r-R)}{R^2} (OAO)_{LL'} \times \frac{\delta(r'-R)}{R^2} Y_L(\hat{r}'), \quad (A2)$$

where the matrix O has its matrix element $O_{LL'}$ defined implicitly in Eq. (A1), and the matrix A has its matrix element $A_{LL'}$ defined implicitly by

$$A(\vec{r}, \vec{r}') = \sum_{LL'} Y_L(\hat{r}) A_{LL'}(R) Y_L(\hat{r}'), \quad |\vec{r}| = |\vec{r}'| = R. \quad (A3)$$

The proof is straightforward. Putting the unit operator $\int dr |\vec{r}\rangle \langle \vec{r}|$ between the operators $\hat{O}\hat{A}\hat{O}$, carrying out the integrations, and using the properties of the δ functions and the orthonormal properties of Y_L , we obtain the expression in Eq. (A2).

(b) For \hat{O} defined in Eq. (A1), the expression

$$\langle \vec{r} | \hat{A}\hat{O}\hat{B} | \vec{r}' \rangle = \sum_{LL'} Y_L(\hat{r}) (AOB)_{LL'} Y_L(\hat{r}') \quad (A4)$$

is also true for $|\vec{r}| = |\vec{r}'| = R$. Here B is defined similarly to A in Eq. (A3). The proof is also similar to that for Eq. (A2).

(c) Most matrix equations used in Sec. IV are direct consequences of Eqs. (A2) and (A4). One example is Eq. (4.6). The averaged Green function $\langle G \rangle$ is defined as $(z - H_0 - \hat{\sigma})^{-1}$, where H_0 is the empty lattice Hamiltonian, and the self-energy $\hat{\sigma}$ can be decomposed into site contributions, $\hat{\sigma} = \sum_n \hat{\sigma}_n$. Define $P = (z - H_0)^{-1}$ and $z = E + i0$; then

$$\langle G \rangle = P + P\hat{\sigma}P + P\hat{\sigma}P\hat{\sigma}P + \dots = \sum_k (P^k + P^k\hat{\sigma}_0P^k + P^k\hat{\sigma}_0P^k\hat{\sigma}_0P^k + \dots), \quad (A5)$$

where P^k is the outgoing KKR Green's function in operator form and the sum is over the first Brillouin zone. Explicitly, we have

$$P^k(\vec{r}, \vec{r}') = \frac{N}{\Omega} \sum_{\vec{g}} \frac{\exp[i(\vec{k} + \vec{g}) \cdot (\vec{r} - \vec{r}')] }{E + i0 - |\vec{k} + \vec{g}|^2}, \quad (A6)$$

where \vec{g} is a reciprocal-lattice vector. Note that in Eq. (A5) only the self-energy at site zero $\hat{\sigma}_0$ is involved. Note also that $\hat{\sigma}_0$ has the property of Eq. (A1). If we take the matrix element in Eq. (A5) in coordinate space with $|\vec{r}| = |\vec{r}'| = R$, we get

$$\begin{aligned}
 \langle G(\vec{r}, \vec{r}') \rangle &= \sum_k \sum_{LL'} Y_L(\vec{r}) (P^k + P^k W P^k \\
 &\quad + P^k W P^k W P^k + \dots)_{LL'} Y_{L'}(\vec{r}') \\
 &= \sum_{LL'k} Y_L(\vec{r}) [P^k (1 - W P^k)^{-1}]_{LL'} Y_{L'}(\vec{r}')
 \end{aligned}
 \tag{A7}$$

where P^k has matrix elements defined in Eq. (4.5). The last step in Eq. (A7) serves to define the matrix G that appears in Eq. (4.6).

*Present address: Department of Physics, Case Western Reserve University, Cleveland, Ohio 44106.

¹Paul Soven, Phys. Rev. **156**, 809 (1967).

²B. Velický, S. Kirkpatrick, and H. Ehrenreich, Phys. Rev. **175**, 747 (1968).

³Paul Soven, Phys. Rev. B **2**, 4715 (1970).

⁴L. Schwarz, F. Brouers, A. V. Vedyayev, and H. Ehrenreich, Phys. Rev. B **4**, 3383 (1971).

⁵J. L. Beeby, Phys. Rev. **135**, A130 (1964); Paul Soven, Phys. Rev. **151**, 539 (1966).

⁶A.-B. Chen, G. Weisz, and A. Sher, Phys. Rev. B **5**, 2897 (1972).

⁷Equations (2.2) and (2.4) correspond to Eqs. (2.7) and (2.22) of Ref. 2, respectively. Note that Eq. (2.4) holds for general localized potentials.

⁸A comparison of the CPA and other single-site approximations in terms of moments and other relevant alloy parameters is summarized by L. Schwartz and E. Siggá, Phys. Rev. B **5**, 283 (1972).

⁹Equation (4.30) of Ref. 2.

¹⁰A.-B. Chen, Bull. Am. Phys. Soc. **17**, 325 (1972).

¹¹Equation (13) of Ref. 1, or Eq. (16) of Ref. 3.

¹²For the discussion of the effect of the excluded terms of the multiple scattering series, see R. M. More, in *Electronic*

Density of States, edited by L. H. Bennett, U. S. Natl. Bur. Std. Spec. Publ. No. 323 (U. S. GPO, Washington, D. C., 1972), p. 515.

¹³Y. Onodera and Y. Toyozawa, J. Phys. Soc. Jap. **24**, 341 (1968), especially Eq. (2.11A).

¹⁴For example, the simple interpolation formula of Lagrange can be used. See H. Margenau and G. M. Murphy, in *The Mathematics of Physics and Chemistry* (Van Nostrand, Princeton, N.J., 1961), Sec. 13.3. Note that Eq. (3.12) corresponds to a linear Lagrange formula.

¹⁵The CPA self-energy has a pole at $E = \epsilon$ for the case $x = 0.15$ and $\delta = 1.5$. The behavior of the self-energy as a function of E is very similar to that shown in Fig. 5(c) of Ref. 2.

¹⁶(S.9) means Soven's Eq. (9) in Ref. 3. The same notation will be used throughout.

¹⁷The Y_L is the same as Y_{ij} in F. G. Ham and B. Segall, Phys. Rev. **124**, 1786 (1961).

¹⁸The structure factors in Eq. (4.5) are the ones that appeared in Ref. 17.

¹⁹This type of sum in Eq. (4.5) is an essential task in all the CPA procedures. It also appeared in the other CPA formalism for muffin-tin potentials; for example, B. L. Gyorffy, Phys. Rev. B **5**, 2382 (1972), Eq. (16).

Interpolation-Scheme Calculation of Electron-Phonon Interaction in Noble and Transition Metals: Copper*

Shashikala G. Das

Argonne National Laboratory, Argonne, Illinois 60439
and University of Chicago, Chicago, Illinois 60637

(Received 14 July 1972)

A simple method for evaluating the electron-phonon interaction matrix elements, and hence the point-mass enhancement and the relaxation time of quasiparticles, is proposed for the transition metals. The method is based essentially on the Bloch model of the electron-phonon interactions and is similar to a pseudopotential formulation with modification to account for the presence of d electrons in the conduction bands and the resulting anisotropy of the above quantities. The results obtained by applying our theory to copper, based on the combined interpolation scheme with explicit inclusion of the screening effects based on Lindhard's formulation and of the contributions from transverse and longitudinal phonons and from umklapp processes, are in fair quantitative agreement with those obtained from a phenomenological interpretation of the experimental cyclotron-mass data of Lee and with the calculations of Nowak based on an empirical phase-shift formulation.

I. INTRODUCTION

Although the importance of the electron-phonon interaction has been well demonstrated in superconductivity,¹ very little work has been done to demonstrate explicitly the nature and anisotropy

of the electron-phonon interaction in transition metals. This is primarily due to the great complexity that the presence of the d bands near the conduction bands in such metals leads to. In simple metals the conduction bands, consisting essentially of s bands, are separated from the well-